Title: Steady-state equilibrium phase inversion recovery ON-resonant water suppression (IRON) MR angiography in conjunction with superparamagnetic nanoparticles. A robust technique for imaging within a wide range of contrast agent dosages.
Authors: Gitsioudis G, Stuber M, Arend I, Thomas M, Yu J, Hilbel T, Giannitsis E, Katus HA, Korosoglou G
Journal: Journal of magnetic resonance imaging : JMRI
Year: 2013 Oct
Volume: 38
Issue: 4
Pages: 836-44
DOI: 10.1002/jmri.24043

Published in final edited form as:
J Magn Reson Imaging. 2013 October ; 38(4): 836–844. doi:10.1002/jmri.24043.

Steady-State Equilibrium Phase Inversion Recovery ON-resonant Water Suppression (IRON) Magnetic Resonance Angiography in Conjunction with Superparamagnetic Nanoparticles. A Robust Technique for Imaging within a Wide Range of Contrast Agent Dosages

Gitsios Gitsioudis, MD[1], **Matthias Stuber, PhD**[2,3], **Ingolf Arend**[1], **Moritz Thomas**[4], **Jing Yu, PhD**[2], **Thomas Hilbel, MD**[1,4], **Evangelos Giannitsis, MD**[1], **Hugo A. Katus, MD**[1], and **Grigorios Korosoglou, MD**[1]

[1]University of Heidelberg, Department of Cardiology, Heidelberg, Germany [2]Russell H. Morgan Department of Radiology and Radiological Sciences, Division of MR Research, Johns Hopkins University School of Medicine, Baltimore, Maryland, USA [3]Center for Biomedical Imaging (CIBM), University Hospital Lausanne, Switzerland [4]University of Applied Sciences Gelsenkirchen, Department of Physical Engineering, Gelsenkirchen, Germany

Abstract

Objectives—To investigate the ability of inversion recovery ON-resonant water suppression (IRON) in conjunction with P904 (superparamagnetic nanoparticles which consisting of a maghemite core coated with a low-molecular-weight amino-alcohol derivative of glucose) to perform steady-state equilibrium phase magnetic resonance angiography (MRA) over a wide dose range.

Materials and Methods—Experiments were approved by the institutional animal care committee. Rabbits (n=12) were imaged at baseline and serially after the administration of 10 incremental dosages of 0.57–5.7 mgFe/Kg P904. Conventional T_1-weighted and IRON MRA were obtained on a clinical 1.5-T scanner to image the thoracic and abdominal aorta, and peripheral vessels. Contrast-to-noise ratios (CNR) and vessel sharpness were quantified.

Results—Using IRON MRA, CNR and vessel sharpness progressively increased with incremental dosages of the contrast agent P904, exhibiting constantly higher contrast values than T_1-weighted MRA over a very wide range of contrast agent doses (CNR of 18.8±5.6 for IRON versus 11.1±2.8 for T_1-weighted MRA at 1.71 mgFe/kg, p=0.02 and 19.8±5.9 for IRON versus −0.8±1.4 for T_1-weighted MRA at 3.99 mgFe/kg, p=0.0002). Similar results were obtained for vessel sharpness in peripheral vessels, (Vessel sharpness of 46.76±6.48% for IRON versus 33.20±3.53% for T_1-weighted MRA at 1.71 mgFe/Kg, p=0.002, and of 48.66±5.50% for IRON versus 19.00±7.41% for T_1-weighted MRA at 3.99 mgFe/Kg, p=0.003).

Conclusion—Our study suggests that quantitative CNR and vessel sharpness after the injection of P904 are consistently higher for IRON MRA when compared to conventional T_1-weighted MRA. These findings apply for a wide range of contrast agent dosages.

Address for correspondence: Grigorios Korosoglou, MD, University Hospital of Heidelberg, Department of Cardiology, Im Neuenheimer Feld 410, 69120 Heidelberg, Germany, grigorios.korosoglou@med.uni-heidelberg.de, Tel: +49 (0)6221 56 37764, Fax: +49 (0)6221 56 4130.

Introduction

Contrast-enhanced magnetic resonance angiography (MRA) is an imaging technique which aids the diagnosis of peripheral, carotid and coronary artery disease in a multitude of clinical settings[1–3]. The short intravascular half-life time of clinically used low-molecular weight gadolinium chelates, however, limits the imaging time window and therefore the spatial resolution of the resultant images[4–6]. Furthermore, the use of gadolinium based contrast agents was recently linked to nephrogenic systemic fibrosis, limiting their applicability in certain patient groups[7,8].

Depending on particle size, surface structure and other factors, superparamagnetic nanoparticles on the other hand, remain in the vascular space for prolonged periods of time, permitting the acquisition of high spatial resolution MRA[9–11]. In this regard, we and others have recently demonstrated the ability of off-resonance imaging techniques including 'Off-Resonance Contrast Angiography' (ORCA) and 'Inversion Recovery with ON-Resonant water suppression' (IRON) to provide signal-enhanced visualization of blood vessels and simultaneously suppress background signal, obviating the need for image subtraction[12–14]. Due to (1) the long half-life time of superparamagnetic nanoparticles in the blood-pool, and (2) the very high signal obtained both from T_1-shortening and from off-resonant protons, IRON MRA was shown to be well-suited for 3D imaging, which inherently allows prolonged scanning times[13,14]. However, in previous studies, the doses of ultrasmall superparamagnetic nanoparticles injected in animals were much higher than the recommended clinical dose of up to 4 mgFe/Kg in humans which is equivalent to 9.5% of total body iron for females and 8% for males, equaling the iron load of 1–2 blood units[15,16].

Therefore, our purpose was to investigate the feasibility of IRON in conjunction with superparamagnetic nanoparticles for contrast-enhanced MRA within a range of dosages applicable for humans. Experiments were performed in rabbits, aiming at the visualization of the thoracico-abdominal aorta as well as of small peripheral arteries, and the resultant IRON MRA images were compared to conventional T_1-weighted acquisitions.

Materials and Methods

Animals and Contrast Agents

The studies were approved by our local institutional animal care and use committee (Karlsruhe, Baden-Württemberg, Germany). Experiments were conducted in 12 rabbits (3.2–4.0 kg), which intramuscularly received ketamine (50 mg/kg) and xylazine (20 mg/dl) for general anaesthesia during the imaging studies. Superparamagnetic nanoparticles contrast material (P904) was provided by Guerbet (Villepinte, France). P904 consists of a maghemite core, which is coated with a low-molecular-weight amino-alcohol derivative of glucose[17]. Its coating represents approximately 2000 hydroxyl groups per nanoparticles (particle size of 21 nm). P904 shows higher relaxivities r_1 and r_2 (14 and 87 $mM^{-1}sec^{-1}$) as the reference-standard contrast agent ferumoxtran-10, measured in water at 1.42 T and 37°C[17]. The highest dose of USPIO contrast material applicable for imaging in humans is 4 mg Fe/kg of body weight[15,18,19]. The plasma half-life for P904 has shown to be 3.5 h in rabbits, which is markedly lower than that of ferumoxtran-10 which is 24–72 h[17]. The lowest dose of superparamagnetic nanoparticles, visible by MRI was reported to be in the order of $10^{13–14}$ iron oxide particles / gram tissue for Monocrystalline Iron Oxide Nanocompounds (MION), which would correspond to an intravenous iron administration of ~0.4–0.6mgFe/Kg[20]. Based on these data, in our study a total dose of 5.7 mg Fe/Kg was administrated in ten incremental steps, i.e. each of 0.57 mgFe/Kg. Imaging was performed at baseline and after the administration of each incremental dosage of the contrast agent (flow diagram illustrated in Figure 1). Venous blood was obtained from all rabbits before and after

contrast material application for biochemical analysis of kidney (creatinine) and hepatic function (transaminase) and cardiac necrosis parameters (creatine kinase, high-sensitive Troponin T, Table 1).

Magnetic Resonance Angiography (MRA)

MR imaging was performed on a 1.5-T clinical scanner (Intera Achieva; Philips Healthcare, Best, The Netherlands) using a 32-element cardiac phased-array receiver coil. Images were obtained at baseline and serially after the administration of incremental dosages of 0.57 mgFe/Kg P904 (Figure 1). For all imaging procedures, volume shimming was used. Scans were performed without parallel imaging, because such techniques would not allow for accurate assessment of SNR and CNR in the resultant images.

(1) Conventional T_1-weighted MRA—For T_1-weighted MRA three-dimensional gradient-echo (fast-field-echo, FFE) images were obtained using the following parameters[13]: Time Repetition/Time Echo (TR/TE)=25/4.5 ms, flip angle (FA)=20°, field-of-view (FOV)=200×150, acquired voxel size 0.5×0.5×1.0 mm^3 and 400×300 image matrix. 70 coronal slices were acquired within a total scan duration of 4 min, resulting in a total volume thickness of 7 cm.

(2) IRON MRA—For IRON MRA, an on-resonant frequency-selective IRON suppression prepulse with BW_{IRON} of 100 Hz, a duration of τ=50 msec and an excitation angle α_{IRON} of 100° was used, as described previously[13]. Conventional fat saturation was achieved by applying a prepulse preceding the IRON prepulse with a −220 Hz frequency offset, a 100 Hz bandwidth, and a 105° FA. Imaging parameters were: TR/TE=5.3/2.0 ms, FA=20°, FOV=120×130 mm, acquired voxel size=0.5×0.5×2.0 mm^3 and 248×254 image matrix. 30 coronal slices were acquired within a total scan duration of 5 min, resulting in a total volume thickness of 6 cm.

MRA Image Analysis

Image analysis was performed with the Soapbubble software tool (Release 5.1 for PRIDE V4.*+V5, Philips Healthcare, Best The Netherlands), as described previously[21]. Signal-to-noise (SNR) and contrast-to-noise ratios (CNR) were calculated *in vivo* by placing regions of interest (ROIs) in the background, in the aortic lumen and in adjacent muscle tissue using original, reformatted magnitude images. For MRA of the thoracic aorta three ROIs were drawn in the ascending aorta, aortic arch and descending aorta, respectively (Figure 2). For MRA of the abdominal aorta and peripheral vessels, also three ROIs were drawn in the suprarenal, and infrarenal aorta, and at the iliacal bifurcation (Figure 2). Vessel sharpness was quantified in the common iliac arteries ~20 mm distal from the aortic bifurcation.

Care was taken to standardize ROI size and placement for better comparison between image sets. The size of the ROI in arbitrary units was 71.45±14.72 for ROI placed in vessels, 75.71±18.43 for ROI placed in the adjacent muscle and 7343.61±1548.22 for ROI placed in the background.

SNR and CNR were calculated using the following equations[21]: $SNR = (I_{Blood})/\mathrm{SDEV}_{\mathrm{Air}}$ and $CNR = (I_{Blood} - I_{Muscle})/\mathrm{SDEV}_{\mathrm{Air}}$. Vessel sharpness was calculated using the equation[22]: $\mathrm{sharpness}^{\pm 1} = \frac{\sum_{i=1}^{N} \mathrm{Edge}\left[i, \vec{p}^{\pm 1}_{Deriche}\right]}{N}$, where i represents the index of each point at the vessel wall, *Edge* the step size of the function at the step position, N the number of edge points, and p the user defined drawing point along the vessel. Besides SNR and CNR analysis, vessel sharpness enables the quantification of vessel conspicuity and is based on a

derivative of the image. On such derivative images, the local signal intensity at the vessel border is a measure of edge definition or signal intensity change relative to the vessel surroundings.

Statistical Analysis

Data are presented as means ± one standard deviation. Differences in SNR, CNR and vessel sharpness between T_1 weighted and IRON-MRA for the same doses of contrast agent were evaluated using 2-tailed unpaired t-tests. Calculations were performed using statistical software (MedCalc® Software, Version 11.4.2.0, Mariakerke, Belgium). For estimation of inter- and intra-observer variability 20 randomly selected cases were analyzed by two independent observers in terms of SNR, CNR and vessel sharpness. Readings were separated by 4 weeks to minimize recall bias. Differences were considered statistically significant at $p<0.05$.

Results

Representative examples of the rabbit thoracic and abdominal aorta imaged during incremental dosages of P904 using T_1-weighted and IRON MRA can be appreciated in Figures 3 and 4. Corresponding images of the aorta at the level of the aortic bifurcation are shown in Figure 5.

For conventional T_1-weighted MRA, CNR and vessel sharpness initially increased after injection of P904 both in the thoracico-abdominal aorta and in peripheral vessels up to a dosage of 1.14 mgFe/kg (SNR (CNR) of 14.9±4.57 (9.0±2.8) for IRON versus 20.9±4.75 (10.9±2.8) for T_1-weighted MRA, p=0.23 and vessel sharpness of 44.9±6.0% for IRON versus 32.7±6.3% for T_1-weighted MRA, p=0.003, at 0.57 mgFe/Kg). Subsequently, SNR, CNR and vessel sharpness decreased with further increasing dosages (Figure 6A–C).

In contrast, using IRON MRA, SNR, CNR and vessel sharpness progressively increased with incremental dosages of the contrast agent P904, exhibiting constantly higher contrast values than T_1-weighted MRA over a very wide range of the clinically applicable dosages (CNR of 18.8±5.6 for IRON versus 11.1±2.8 for T_1-weighted MRA at 1.71 mgFe/kg, p=0.02 and 19.8±5.9 for IRON versus −0.8±1.4 for T_1-weighted MRA at 3.99 mgFe/kg, p=0.0002), (Figure 6B). Similar results were observed for vessel sharpness in peripheral vessels, where IRON-MRA also exhibited constantly higher values than T_1-weighted MRA within the clinically applicable dosage range (vessel sharpness of 46.76±6.48% for IRON versus 33.20±3.53% for T_1-weighted MRA at 1.71mgFe/Kg, p=0.002, and of 48.66±5.50% for IRON versus 19.00±7.41% for T_1-weighted MRA at 3.99 mgFe/Kg, p=0.003), (Figure 6C).

Observer Variabilities

Quantification of SNR, CNR and vessel sharpness were reproducible exhibiting low intra- and interobserver variabilities of 8.1%, and 4.2% for SNR, 8.9% and 5.2% for CNR and 4.6% and 4.2% for vessel sharpness, respectively.

Discussion

To our knowledge, this is the first study that demonstrates the feasibility of inversion recovery ON-resonant water suppression (IRON) imaging in conjunction with superparamagnetic nanoparticles (P904) for steady-state equilibrium phase MRA *within a wide range of dosages applied in human studies*[15,18]. IRON MRA exhibited very high contrast between the blood-pool and the surrounding tissue without the need for image subtraction. The vessel conspicuity provided by IRON MRA surpassed that provided by

conventional T_1-weighted techniques in terms of SNR, CNR and resultant vessel sharpness. These effects remained constant over a wide range of contrast agent dosages resulting in very robust contrast behavior.

Several non-contrast and contrast enhanced angiography techniques have been previously described, aiming at the visualization of peripheral or coronary vessels. Contrast enhanced MRA on the other hand, depends on intravenous application of contrast material and is a robust imaging technique with a multitude of clinical applications[23]. Gadolinium (Gd)-based contrast agents are routinely used for contrast-enhanced MRA, increasing vascular conspicuity by decreasing the T_1-relaxation time of blood. However, the short arterial imaging window before intravenous and extracellular distribution consecutively results in a short arterial imaging window which governs the maximum spatial resolution and blood-tissue contrast that can be obtained[24,25].

In the present study we demonstrated for the first time the ability of the IRON technique in conjunction with superparamagnetic nanoparticles, administrated *within the range of the dose applied in human clinical studies* to visualize blood vessels with high spatial resolution in an experimental rabbit model. The prolonged intravascular plasma half-life of P904 allowed for 3D T_1-weighted acquisitions with high spatial resolution and CNR. However, in agreement with theoretical considerations, competing T_2^* effects due to susceptibility effects are unavoidable with increasing dosages of P904, even with ultra-short echo times[26,27]. This resulted in increasing signal void within the vessels of interest causing decreased SNR, CNR and vessel sharpness with increasing P904 doses in our study. IRON MRA on the other hand, provided high intravascular SNR after P904 administration, which, in conjunction with the simultaneous background suppression resulted in very high intravascular contrast. Thus, intravascular contrast was ~60% higher for IRON compared to T_1-weighted MRA after the administration of clinically applicable contrast agent doses up to 4.0 mg Fe/Kg. This is attributable to the dual origin of positive signal originating both from off-resonant protons and from T_1 recovery[14]. Furthermore, vessel sharpness was markedly higher in the aorta with IRON than in conventional T_1-weighted MRA in all applied concentrations of P904. In the past the IRON sequence was used in combination with the long-circulating monocrystalline iron oxide nanoparticle (MION)-47 for contrast material–enhanced magnetic resonance (MR) angiography by Korosoglou et al.[13]. Using 1.27 mgFe/Kg or 3.96 mgFe/Kg of MION-47 and comparing with conventional T_1-weighted MRA they showed that IRON MRA provides high intravascular contrast over a long time and without the need for image subtraction. It remains to be elucidated in future studies whether conventional T_1-weighted or IRON MRA is the adequate choice.

As previously described the minimum of signal intensity with IRON MRA depends on tissue characteristics and the vessel orientation relative to the main magnetic field[14]. As a result, edge enhancement effects occur in vessels perpendicular to the fold-over-direction as shown in Figure 4, which may have led to an overestimation of the acquired vessel sharpness. However, vessel conspicuity was similar between the aorta and the renal artery, while computation of vessel sharpness in the latter would have been hindered by the close proximity of the renal veins.

Potential (pre-) clinical applications

Because of the very high intravascular signal obtained by IRON MRA, this modality may provide adequate signal in very small vessels as shown for peripheral iliac rabbit arteries in our study, which may not be detectable using conventional MR-techniques. This may be useful for the evaluation of small collateral vessels, in the progress of arteriogenesis or for the monitoring of angiogenesis suppression therapies in cancer. The clinical application of IRON off-resonance angiography may be limited by frequency shift and edge enhancement

in vessels with extreme tortuosity. The dual origin of signal enhancement with IRON however, originating from both off-resonant protons and T_1-recovery, the latter being orientation independent, may help to circumvent such limitations. Whether a broad application of IRON off-resonance angiography in clinical realm may be limited by the induced frequency shift and edge enhancement remains to be elucidate in future studies.

Furthermore, as coronary MRA remains a challenging task for clinical routine applications. Due to the relation between scan time and SNR, the fact that IRON MRA provides higher signal compared to conventional techniques (originating both from off-resonant protons and from T_1-recovery) may be exploited to further reduce scan time for MRA in such future experiments. The fact that our observations were obtained using a clinical 1.5 T scanner, and using P904, a contrast agent similar to ferumoxtran (particle size 30–35 nm, plasma half-life 24–30 hours) both indicate translational potential for human use. In this regard, ferumoxytol is currently clinically approved for iron-replacement treatment in patients with chronic renal failure[28,29]. Additional, improvement in signal intensity could be achieved using a 3.0 T scanner[20]. Furthermore, in contrast to gadolinium-based contrast agents, nephrogenic systemic fibrosis has not been described in superparamagnetic nanoparticles. However, minor changes in PTT (partial thromboplastin time) have been described for iron-based contrast agents without leading to clinically significant bleeding. Such changes were attributed to a transient decrease in factor XI activity[30]. In general, USPIOs are well tolerated without significant side effects in human trials[31]. Thus, in patients with renal failure such nanoparticles may represent a valuable alternative for contrast-enhanced MRA[32].

Our study has some limitations. The number of animals studied was relatively small. However, the magnitude of contrast enhancement was very similar among animals as evidenced by the small standard deviation of all quantitative measurements. In addition, contamination of the venous blood pool after the administration of superparamagnetic nanoparticles cannot be avoided by IRON MRA. But this represents a general problem with steady state MRA, where the discrimination of neighboring arteries and veins may be impaired. Besides, as previously described by Vonken et al. edge enhancement effects in the fold-over direction occur dependent on the vessel orientation relative to the main magnetic field. This indeed poses a potential limitation for IRON MRA of small or tortuous vessels. Next, long TE resulted during scan protocol optimization possibly due to gradient limitations with our 1.5 Tesla scanner by choosing TE automatically as “shortest”, with similar parameters as were published in previous studies and having activated the flow compensation[13]. This may account for the suboptimal performance of T_1-weighted MRA due to signal loss with increasing T2* values. The spatial resolution of T_1-weighted and IRON MRA was not identical. However, all the imaging parameters including the total scan time, the scan volume and the spatial resolution were optimized experimentally in order to reach optimal image quality for each technique individually. During this developmental phase we aimed at optimizing both vessel conspicuity and spatial resolution for adequate visualization of both the thoracico-abdominal aorta and peripheral arteries. The lower resolution in slice selection direction for in IRON MRA supports higher SNR and CNR values. Last, in humans Hamm et al. recently showed that the SPIO *SHU 555 A* causes a transient increase of aPTT[31]. However, the normal range of aPTT was not exceeded. Such changes were not expected to translate to increased bleeding risk for the patients. However, patients with increased bleeding risk would possibly have to be excluded from such clinical studies in the future. Finally, the fact that the contrast agent we used is not approved for clinical use is a limitation.

In conclusion, IRON MRA provides significantly higher blood-to-tissue contrast both in the aorta and in small peripheral rabbit vessels compared to conventional T_1-weigthed

angiography within the dose range applicable for clinical human use. High CNR and vessel sharpness remain stable over a wide range of contrast agent concentrations, which may possibly allow for more robust MRA acquisitions in clinical applications. Especially, in light of clinical MR setting used in our study and the duration of the IRON MRA acquisitions (~5 min) the translation of our findings to the clinical realm appears promising.

Acknowledgments

Disclosures:

- **i.** The contrast agent P904 was kindly provided by Guerbet (Villepinte, France).
- **ii.** This work was supported by a grant from MSD and in part by the NIH grants R01-HL084186 and ARRA 3R01-Hl084186-04S1.

References

1. Zhang H, Maki JH, Prince MR. 3D contrast-enhanced MR angiography. J Magn Reson Imaging. 2007; 25(1):13–25. [PubMed: 17154188]
2. Yang Q, Li K, Liu X, et al. Contrast-enhanced whole-heart coronary magnetic resonance angiography at 3.0-T: a comparative study with X-ray angiography in a single center. J Am Coll Cardiol. 2009; 54(1):69–76. [PubMed: 19555843]
3. Menke J. Diagnostic accuracy of contrast-enhanced MR angiography in severe carotid stenosis: meta-analysis with metaregression of different techniques. Eur Radiol. 2009; 19(9):2204–2216. [PubMed: 19399505]
4. Yucel EK. MR angiography for evaluation of abdominal aortic aneurysm: has the time come? Radiology. 1994; 192(2):321–323. [PubMed: 8029387]
5. Prince MR. Gadolinium-enhanced MR aortography. Radiology. 1994; 191(1):155–164. [PubMed: 8134563]
6. Grist TM. Future directions of magnetic resonance angiography. Invest Radiol. 1998; 33(9):485–487. [PubMed: 9766031]
7. Kallen AJ, Jhung MA, Cheng S, et al. Gadolinium-containing magnetic resonance imaging contrast and nephrogenic systemic fibrosis: a case-control study. Am J Kidney Dis. 2008; 51(6):966–975. [PubMed: 18501784]
8. Collidge TA, Thomson PC, Mark PB, et al. Gadolinium-enhanced MR imaging and nephrogenic systemic fibrosis: retrospective study of a renal replacement therapy cohort. Radiology. 2007; 245(1):168–175. [PubMed: 17704357]
9. Allkemper T, Bremer C, Matuszewski L, Ebert W, Reimer P. Contrast-enhanced blood-pool MR angiography with optimized iron oxides: effect of size and dose on vascular contrast enhancement in rabbits. Radiology. 2002; 223(2):432–438. [PubMed: 11997549]
10. Frank H, Weissleder R, Brady TJ. Enhancement of MR angiography with iron oxide: preliminary studies in whole-blood phantom and in animals. AJR Am J Roentgenol. 1994; 162(1):209–213. [PubMed: 8273667]
11. Ruehm SG, Corot C, Vogt P, Kolb S, Debatin JF. Magnetic resonance imaging of atherosclerotic plaque with ultrasmall superparamagnetic particles of iron oxide in hyperlipidemic rabbits. Circulation. 2001; 103(3):415–422. [PubMed: 11157694]
12. Edelman RR, Storey P, Dunkle E, et al. Gadolinium-enhanced off-resonance contrast angiography. Magn Reson Med. 2007; 57(3):475–484. [PubMed: 17326177]
13. Korosoglou G, Shah S, Vonken EJ, et al. Off-resonance angiography: a new method to depict vessels--phantom and rabbit studies. Radiology. 2008; 249(2):501–509. [PubMed: 18780823]
14. Vonken EJ, Korosoglou G, Yu J, Schar M, Weissleder R, Stuber M. On the dual contrast enhancement mechanism in frequency-selective inversion-recovery magnetic resonance angiography (IRON-MRA). Magn Reson Med. 2009; 62(2):314–324. [PubMed: 19526511]

15. Li W, Tutton S, Vu AT, et al. First-pass contrast-enhanced magnetic resonance angiography in humans using ferumoxytol, a novel ultrasmall superparamagnetic iron oxide (USPIO)-based blood pool agent. J Magn Reson Imaging. 2005; 21(1):46–52. [PubMed: 15611942]
16. Prince Martin RZHL, Chabra Shalini G, Jacobs Paula, Wang Yi. A pilot investigation of new superparamagnetic iron oxide (ferumoxytol) as a contrast agent for cardiovascular MRI. Journal of X-Ray Science and Technology. 2003; 11:231–240. [PubMed: 22388293]
17. Sigovan M, Boussel L, Sulaiman A, et al. Rapid-clearance iron nanoparticles for inflammation imaging of atherosclerotic plaque: initial experience in animal model. Radiology. 2009; 252(2): 401–409. [PubMed: 19703881]
18. Ersoy H, Jacobs P, Kent CK, Prince MR. Blood pool MR angiography of aortic stent-graft endoleak. AJR Am J Roentgenol. 2004; 182(5):1181–1186. [PubMed: 15100115]
19. Prince MRZH, Chabra SG, Jacobs P, Wang Y. A pilot investigation of new superparamagnetic iron oxide (ferumoxytol) as a contrast agent for cardiovascular MRI. J X-ray sci technol. 2003; 11:231–240.
20. Shen T, Weissleder R, Papisov M, Bogdanov A Jr, Brady TJ. Monocrystalline iron oxide nanocompounds (MION): physicochemical properties. Magn Reson Med. 1993; 29(5):599–604. [PubMed: 8505895]
21. Etienne A, Botnar RM, Van Muiswinkel AM, Boesiger P, Manning WJ, Stuber M. "Soap-Bubble" visualization and quantitative analysis of 3D coronary magnetic resonance angiograms. Magn Reson Med. 2002; 48(4):658–666. [PubMed: 12353283]
22. Botnar RM, Stuber M, Danias PG, Kissinger KV, Manning WJ. Improved coronary artery definition with T2-weighted, free-breathing, three-dimensional coronary MRA. Circulation. 1999; 99(24):3139–3148. [PubMed: 10377077]
23. Yucel EK, Anderson CM, Edelman RR, et al. AHA scientific statement. Magnetic resonance angiography : update on applications for extracranial arteries. Circulation. 1999; 100(22):2284–2301. [PubMed: 10578005]
24. Meaney JF, Ridgway JP, Chakraverty S, et al. Stepping-table gadolinium-enhanced digital subtraction MR angiography of the aorta and lower extremity arteries: preliminary experience. Radiology. 1999; 211(1):59–67. [PubMed: 10189454]
25. Leiner T. Magnetic resonance angiography of abdominal and lower extremity vasculature. Top Magn Reson Imaging. 2005; 16(1):21–66. [PubMed: 16314696]
26. Kroft LJ, de Roos A. Blood pool contrast agents for cardiovascular MR imaging. J Magn Reson Imaging. 1999; 10(3):395–403. [PubMed: 10508301]
27. Loubeyre P, Zhao S, Canet E, Abidi H, Benderbous S, Revel D. Ultrasmall superparamagnetic iron oxide particles (AMI 227) as a blood pool contrast agent for MR angiography: experimental study in rabbits. J Magn Reson Imaging. 1997; 7(6):958–962. [PubMed: 9400837]
28. Besarab, A.; Coyne, D.; Bolton, WK., et al. Ferumoxytol as an intravenous iron replacement therapy: safety results from two phase III studies in subject with chronic kidney diseases (CKD). American Society of Nephrology 40th Annual Meeting and Scientific Exposition; San Francisco. 2007. p p. SUPO805.
29. Sosnovik DE, Nahrendorf M, Weissleder R. Magnetic nanoparticles for MR imaging: agents, techniques and cardiovascular applications. Basic Res Cardiol. 2008; 103(2):122–130. [PubMed: 18324368]
30. Reimer P, Tombach B. Hepatic MRI with SPIO: detection and characterization of focal liver lesions. Eur Radiol. 1998; 8(7):1198–1204. [PubMed: 9724439]
31. Hamm B, Staks T, Taupitz M, et al. Contrast-enhanced MR imaging of liver and spleen: first experience in humans with a new superparamagnetic iron oxide. J Magn Reson Imaging. 1994; 4(5):659–668. [PubMed: 7981510]
32. Neuwelt EA, Hamilton BE, Varallyay CG, et al. Ultrasmall superparamagnetic iron oxides (USPIOs): a future alternative magnetic resonance (MR) contrast agent for patients at risk for nephrogenic systemic fibrosis (NSF)? Kidney Int. 2009; 75(5):465–474. [PubMed: 18843256]

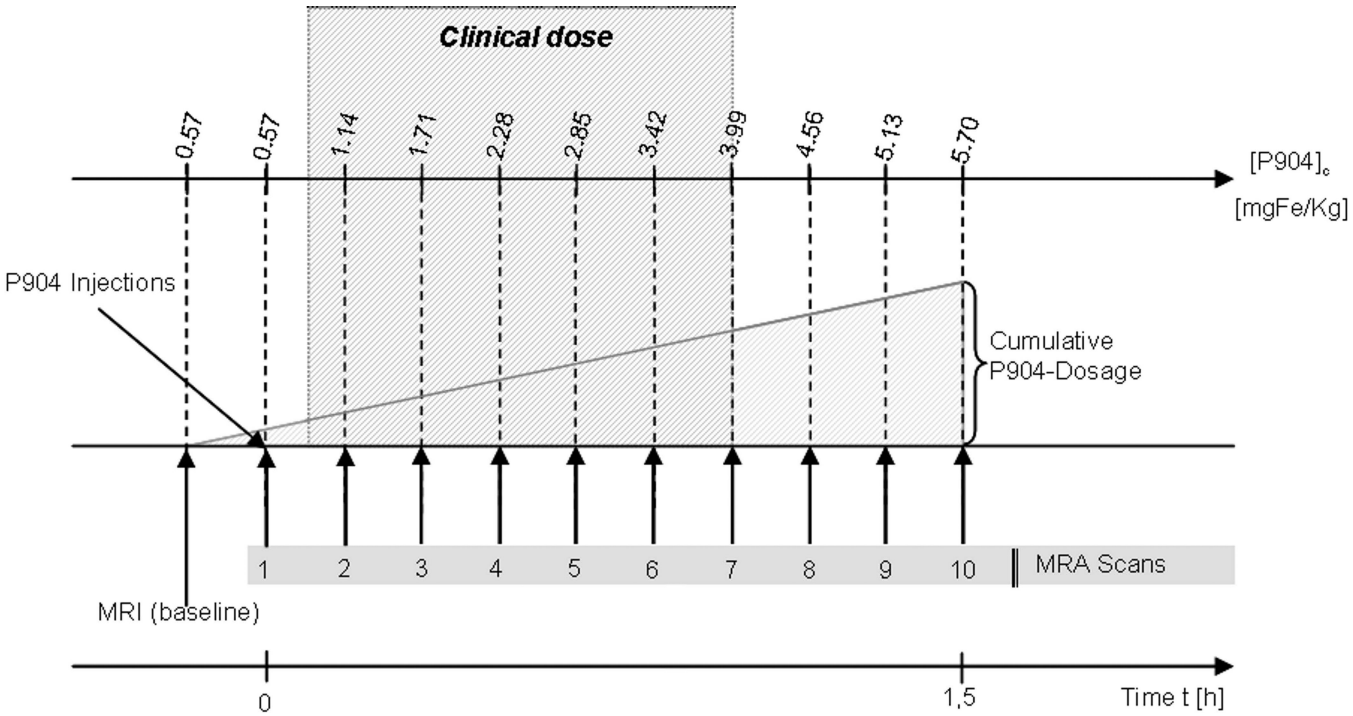

Figure 1.
Schematic illustration of the P904 administration in animal studies.

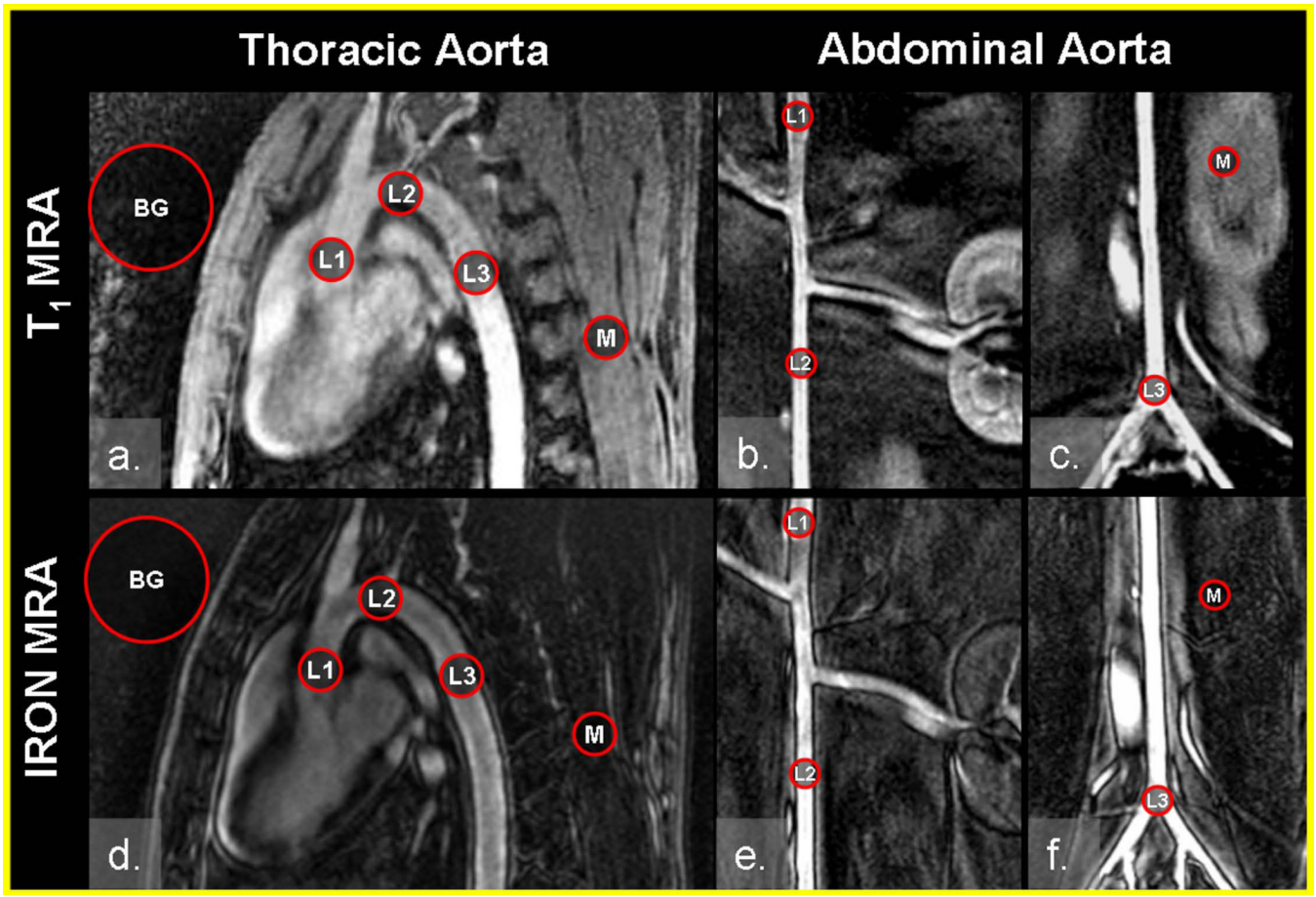

Figure 2.
ROI positioning in the thoracic (a & d) and the abdominal aorta (b–c & e–f) with T_1 MRA (upper row) and IRON MRA images (lower row) for SNR and CNR analysis. BG indicates Background ROI; L1-3, Lumen ROIs and M, Muscle ROI.

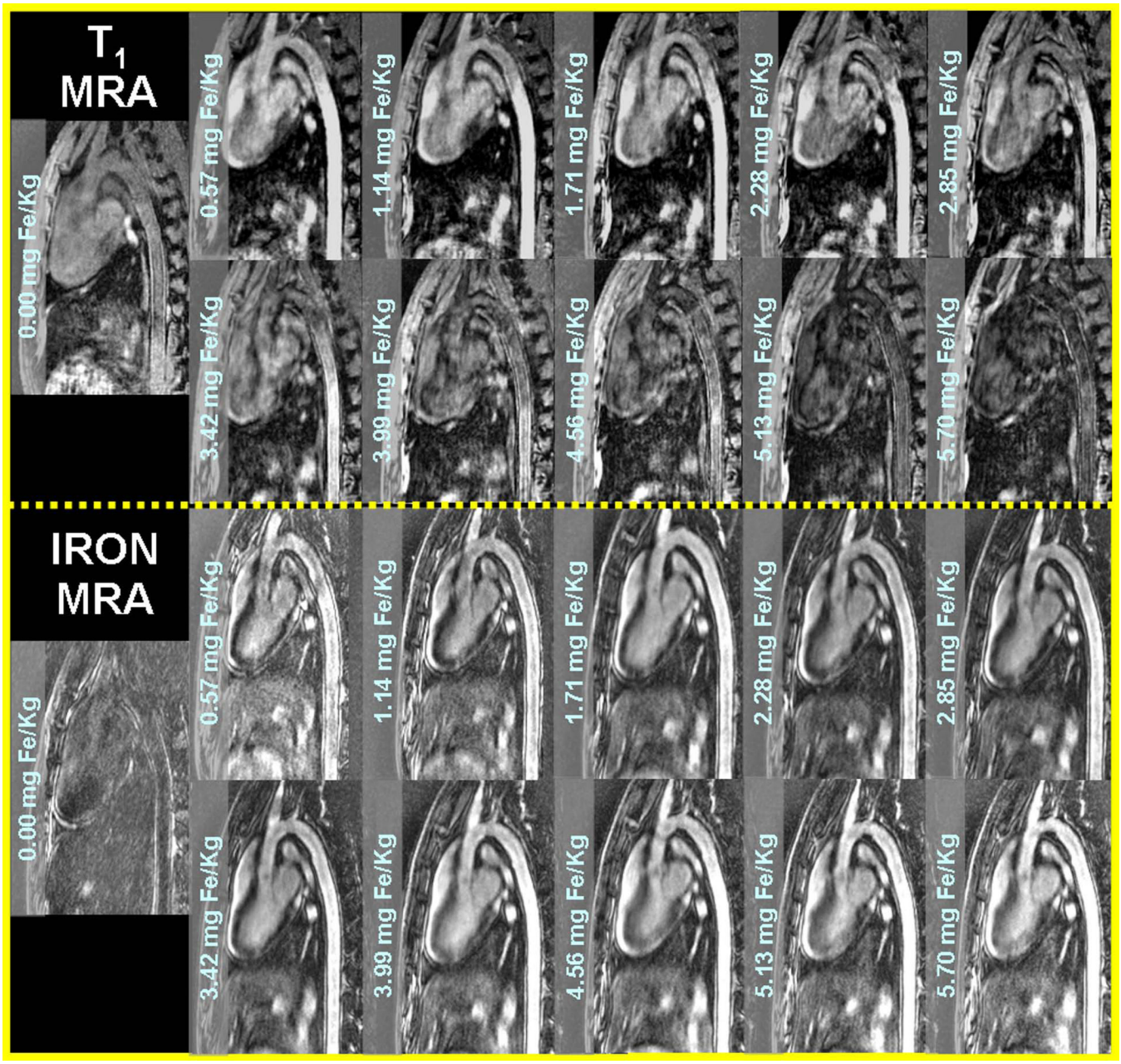

Figure 3.
Representative examples of the rabbit thoracic aorta imaged during incremental dosages of P904 using T_1-weighted and IRON MRA

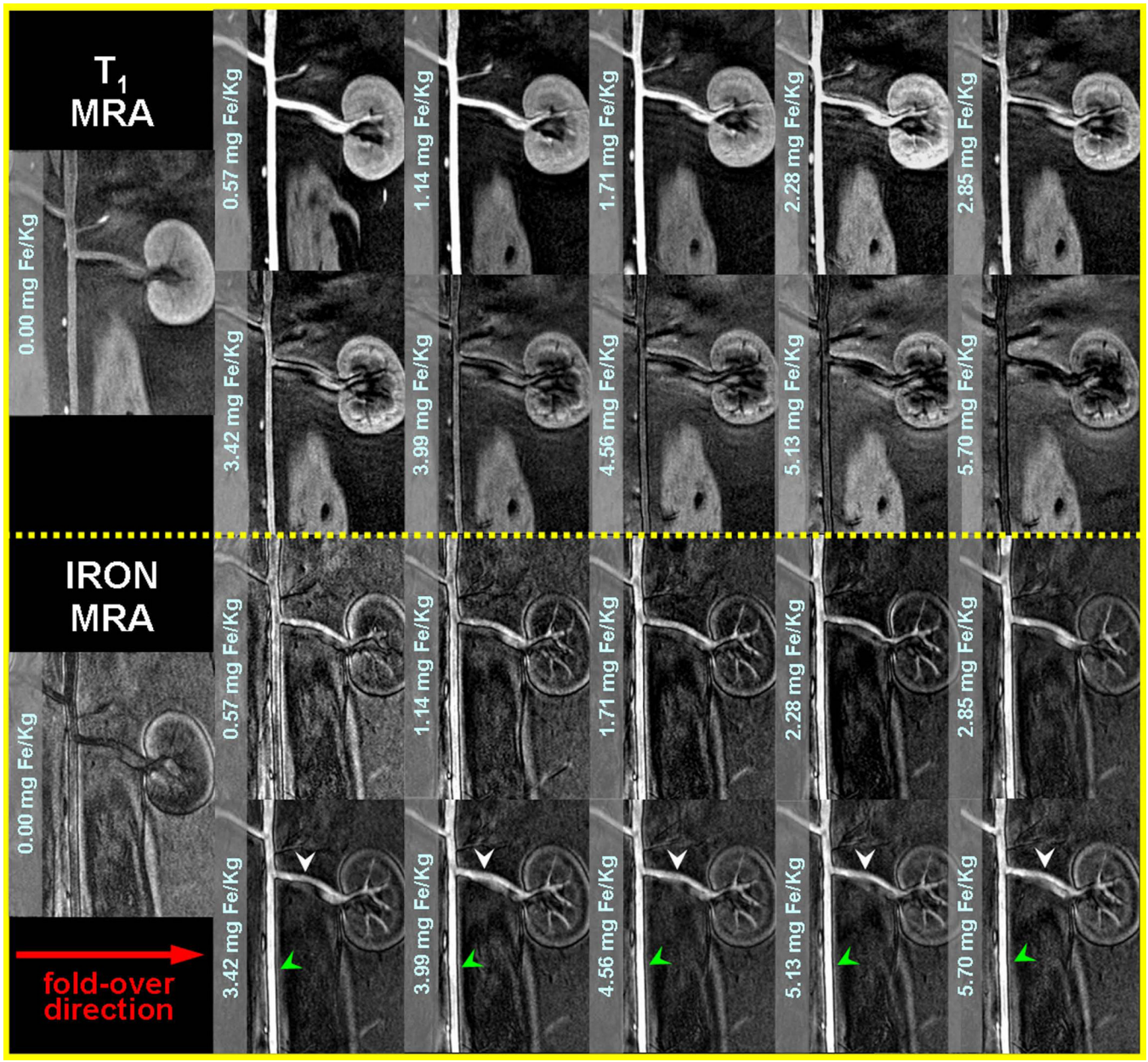

Figure 4.

Representative examples of the rabbit abdominal aorta imaged during incremental dosages of P904 using T_1-weighted and IRON MRA. Edge enhancement effect in the abdominal aorta (green arrows) can be observed perpendicular to the fold-over direction. White arrows indicate the renal vein which is located close to the renal artery.

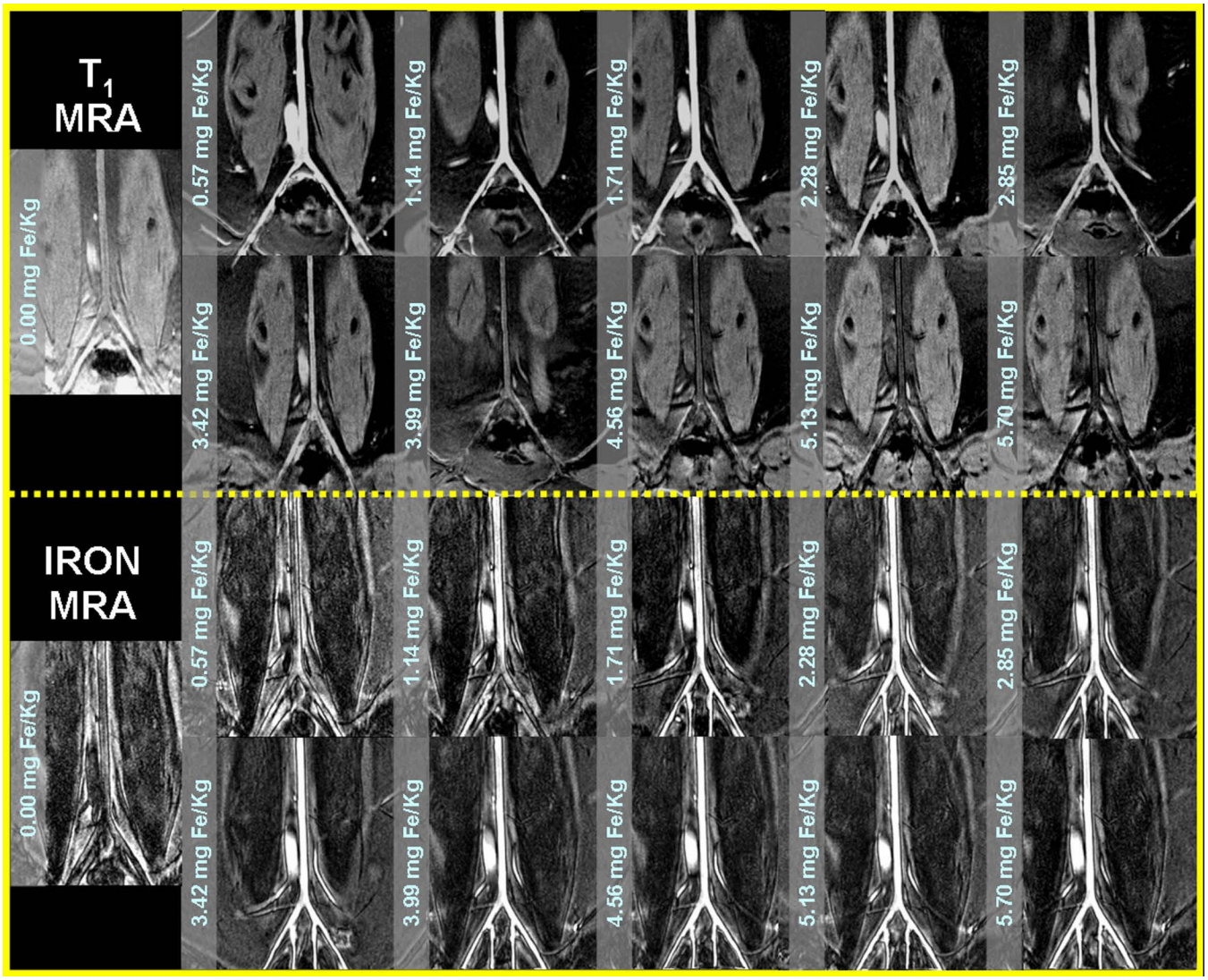

Figure 5.
Representative examples of the rabbit iliac vessels imaged during incremental dosages of P904 using T_1-weighted and IRON MRA.

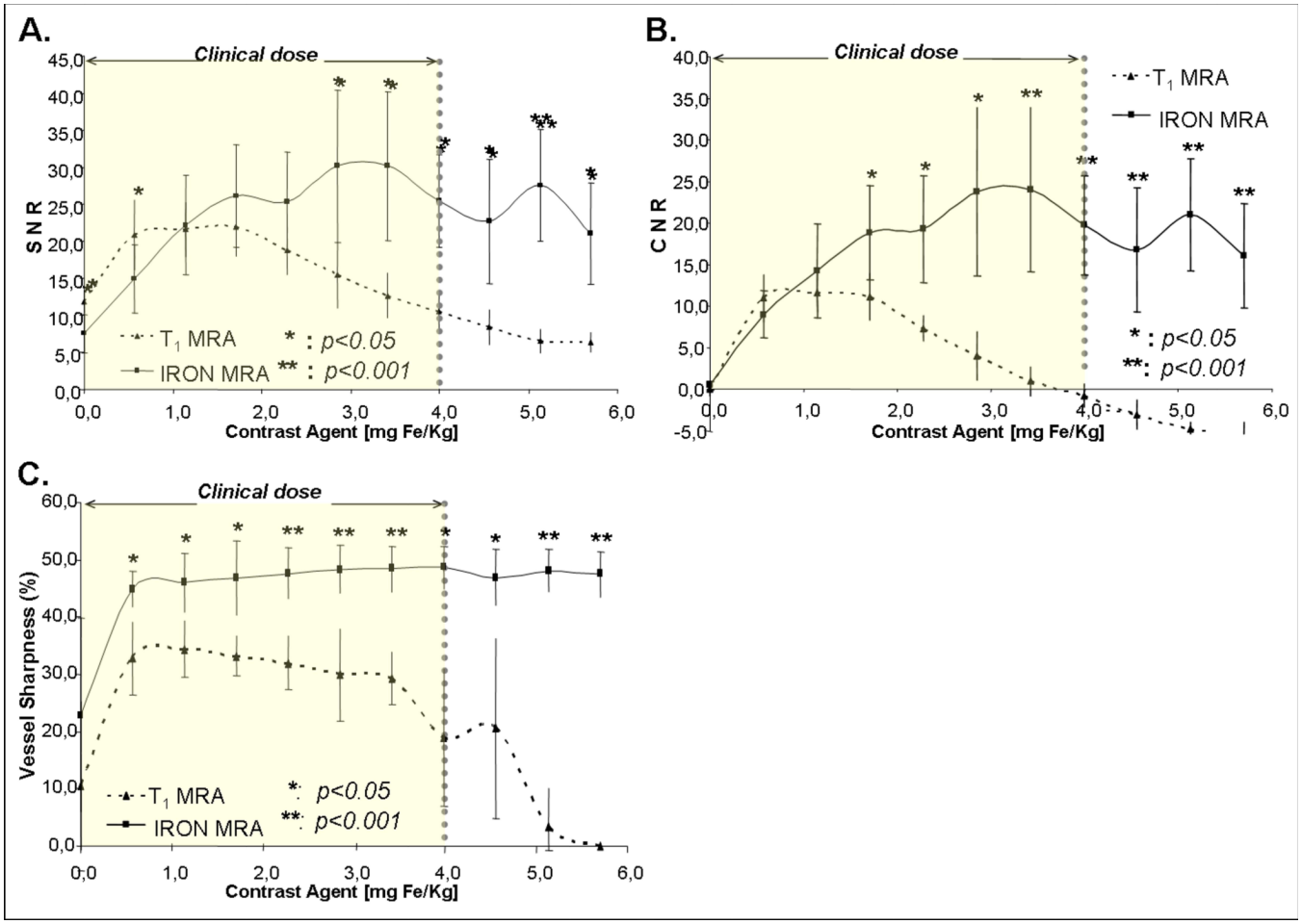

Figure 6.

SNR (A.), CNR (B.) and vessel sharpness (C.) during incremental dosages of P904 and using IRON versus T_1-weighted MRA for imaging.

Table 1

Biochemical analysis (n=12 rabbits) of kidney (creatinine) and hepatic function (transaminase) and cardiac necrosis parameters (creatine kinase, high-sensitive Troponin T) showed no significant difference (value ± standard deviation) before and after contrast material (CM) application.

	Creatinine [mg/dl]	**GOT/AST [U/l]**	**GPT/ALT [U/l]**	**Creatine kinase [U/l]**	**hs-TroponinT [pg/ml]**
before CM	0.7 ± 0.1	32.6 ± 18.5	64.5 ± 40.7	2683.5 ± 1920.2	15.6 ± 6.8
after CM	0.7 ± 0.1	26.9 ± 7.0	80.9 ± 31.5	3090.8 ± 1649.2	9.9 ± 5.8
p-value	0.4	0.3	0.3	0.6	0.1